Interactions between water soluble porphyrin-based star polymer and amino acids: Spectroscopic evidence of molecular binding

Nicola Angelini, Norberto Micali,* and Valentina Villari
CNR–Istituto per i Processi Chimico-Fisici, sez. Messina, Via La Farina 237, I-98123 Messina, Italy

Placido Mineo and Daniele Vitalini
CNR–Istituto di Chimica e Tecnologia dei Polimeri, Viale Andrea Doria 6, I-95125 Catania, Italy

Emilio Scamporrino
Dipartimento di Scienze Chimiche, Universita' di Catania, Viale Andrea Doria 6, I-95125 Catania, Italy
(Received 23 July 2004; published 28 February 2005)

Molecular interactions giving rise to stable complexes between an uncharged water soluble cobalt-porphyrin and amino acids are investigated by time-resolved fluorescence, uv-vis, and circular dichroism measurements. This metalloporphyrin seems to act, by means of the coordination site of the cobalt of the core, as a recognition host, preferentially, with amino acids possessing aromatic groups. The binding with aliphatic amino acids requires longer time scales to be efficient and likely involves a slow kinetic process. The experimental findings suggest that, besides the metal(host)-N(guest) coordination bond, which is the common requisite for all amino acids, a preferential interaction with aromatic groups exists there. The solubility in water of the molecule, guaranteed by the polyethylene glycol arms as peripheral substituents, in the absence of electric charges, allows for a more selective discrimination of the binding process with respect to other water-soluble charged porphyrins. The interest devoted to the porphyrin-based star polymer and its recognition properties is, therefore, founded on the potential use either in polymeric matrices for material science or in aqueous solution for bioscience.

DOI: 10.1103/PhysRevE.71.021915 PACS number(s): 87.64.Ni, 82.70.−y, 39.30.+w, 36.20.Ey

I. INTRODUCTION

In recent years, there has been intense interest in the development and investigation of biofunctional nanoparticles consisting of proteins bounded to carrier units, thanks to their potential use in biomedicine and biotechnology as drug delivery systems, immunoassays, and biocatalysts [1–4]. Similarly, systems that can act as a target for amino acids are fundamental for protein recognition and identification and can be exploited for creating biosensors.

Amino acids (AAs), well-known units in the building of protein molecules, play an unquestionable role in biochemical processes, acting also as an important nutrient. For these reasons, several techniques of identification and analysis of the AAs contained in organic matrices, such as chromatographic (e.g., HPLC and GC) or spectroscopic (based on the chromatic changes of amino acids solutions in the presence of appropriate reactive dyes, such as *p*-benzoquinone, 2,4-dinitrobenzenesulphonic acid or 4-hydroxy-3,5-dimethoxybenzaldehyde) methods, have been developed. However, despite the high sensibility and selectivity achievable, these techniques are often expensive and require relatively high amounts of material and lengthy analysis [4]. Recently, some authors [5–9] have focused their attention on systems containing metal-porphyrin derivatives in which the interactions between metal d-electrons of the porphyrin and some AAs cause spectroscopic changes, thus making possible the recognition of both AAs and oligopeptides or proteins containing them.

The use of porphyrins as AAs sensors is feasible with the active species in solution or immobilized on specific polymeric or inorganic substrates. In this last case, the porphyrin-containing material should also be used for chromatographic separations.

Porphyrins have a great interest also in the biomedical field. As an example, based on the specific affinity of porphyrins with neoplastic cells [10–15], these compounds can be used for the localization and size determination of tumoral tissues. Porphyrin localization is then achieved by means of fluorimeters (based on the fluorescence of the metal-free molecule) or scintillators (introducing a specific radio nuclide into the porphyrin cavity, the so-called "radio-labeling" method). Moreover, the strong photosensitization properties characteristic of the porphyrin compounds permit a localized photodegradative treatment circumscribed of "sick" tissues, thus reducing the damage of the surrounding tissues.

Another interesting application of porphyrins in the biomedical field is related to their peculiarity, both of free and metal complexed species, to inhibit the formation of a protease-resistant protein responsible for the transmissible spongiform encephalopatie [16]. Water solubility is often required in many applications of porphyrin compounds. Actually, this goal is prevailingly obtained inserting some electrically charged groups in the molecule, but this approach can represent a limit in some applications. In the sensor field, for example, the existence of charges in the active molecular sensor can complicate the study of the ''pure" AAs/porphyrin

*Electronic address: micali@me.cnr.it

coupling. Analogously, in clinical trials, the charges can directly interact with cellular membranes hindering the penetration of porphyrins inside the cells [17–19]. Differently, the water solubility of the porphyrins employed in this work is due to the presence of long neutral hydrophilic groups (polyethylene glycols, PEGs) bound to the porphyrin core, which also reduces the typical detrimental aggregation phenomenon of porphyrin units [20]. The recognition capability of these porphyrin systems is due to the insertion of particular metal atoms in the porphyrin core.

In the present work, a three-functional system bearing a porphyrin unit (the chromophore, having a very high molar absorption coefficient), a hydrophilic PEG component (the floaters), and a cobalt atom (the sensor) complexed in the porphyrin core, was examined. In particular, the molecular interaction between porphyrin and amino acids was investigated by means of uv-vis, circular dichroism, and steady-state and time-resolved fluorescence anisotropy. An analogous study was performed also for a more complicated system, in which insulin was added to the cobalt-porphyrin (Co-P) solution. The observed interaction between the Co-P system and the AAs units, both free or inside the protein chain, should allow the use of these systems as an AA sensor.

II. EXPERIMENTAL SECTION

Materials: L- and D-Amino acids (AAs, Kit No. LAA-21) and bovine insulin were obtained from Sigma Chemical Company. Amino acids and insulin used in this work are indicated in the following as L-alanine=L-Ala; L-phenyl-alanine=L-Phe; D-phenyl-alanine=D-Phe; L-Triptophane =L-Trp; insulin=Ins. [*5,10,15,20*-tetrakis-*p*(ω-methoxy-polyethylenoxyphenl)]porphyrin (2H-P), [*5,10,15,20*-tetrakis-*p*(ω-methoxy-polyethylenoxyphenyl)]zinc(II) porphyrin, (Zn-P), and [*5,10,15,20*-tetra-*p*(ω-methoxy-polyethylenoxyphenyl)]cobalt(II) porphyrin, (Co-P), all having an average molecular mass M_n of about 3600 Da (see Fig. 1) were synthesized as described previously [21]. The water solubility of these porphyrin derivatives has been achieved by introducing hydrophylic substituents (polyethylene glycol chains with an M_n value of 750 Da) in the peripheral positions of the hydrophobic porphyrin core, thus obtaining uncharged hydrosoluble molecules.

For a better AAs solubilization in water, the *p*H of the solutions was maintained at about 9 by means of borate buffer (from Metrohm). All porphyrin/AAs mixtures were prepared, to facilitate the host-guest interaction between AAs and porphyrin, with a 1:10 and 1:100 molar ratio for the uv-vis measurements and 1:100 molar ratio for the fluorescence and circular dichroism measurements. For the porphyrin/Ins mixture, the molar ratio used was instead 1:1. The star-polymer concentration was fixed at 46 μM for all the measurements.

All the solutions were freshly prepared and measurements were performed within one hour.

A. Time-resolved fluorescence

All fluorescence measurements were carried out by a time-correlated-single-photon-counting [22] home-made apparatus. An argon-ion laser (Spectra-Physics BeamLok 2080), operating in the mode-locked regime (514 nm) at a repetition rate of 82 MHz, was used to synchronously pump a rhodamine 6G dye laser (Spectra-Physics 375B). The output pulses of the dye laser of ~2 ps full width at half maximum at 575 nm wavelength passed through a Glan-Taylor polarizer (to eliminate any depolarization effects due to the mirrors placed along the laser optical pathway) and then used as an exciting beam focused on the sample. The temperature of the sample was controlled with a 0.1 °C resolution with a Haake C25-F6 thermostat at $T=22$ °C. Part of the dye laser beam was sent to an autocorrelator (Spectra-Physics 409) to check the excitation pulse stability. The fluorescence emission, before being detected, passed through a rotatable analyzer, to select the vertically (I_{VV}) and the horizontally (I_{VH}) polarised fluorescence (the analyzer was removed when total fluorescence decay curves were collected); a long-pass filter with the 50% transmittance at 610 nm, to remove a possible scattered excitation light; and a polarization scrambler, to avoid any effects due to the different transmission efficiency of the monochromator and of the photomultiplier for vertically and horizontally polarized light. The fluorescence photons were detected through a monochromator (Oriel Cornerstone 1/8 m) by a microchannel-plate photomultiplier (Hamamatsu R1645U-01, ~200 ps rising-time) operating in the single-photon counting regime. The photomultiplier pulses, properly preamplified (EG-G Ortec VT120), were processed by a constant fraction discriminator (EG-G Ortec 935), to obtain a timing independent of pulse height variations, and by pulse-delay generator. The output signals of the mode-locker driver, synchronized with the exciting laser pulses, and of the photomultiplier were sent, respectively, to the stop and start inputs of a time-to-amplitude converter (TAC, EG-G Ortec 567). Finally, the output pulses from the TAC were sent to a computer-controlled multichannel analyzer card (EG-G Ortec Trump-8k/2k) operating in the pulse-height-acquisition mode, to record and store the decay curves. Moreover, another output of the constant fraction dis-

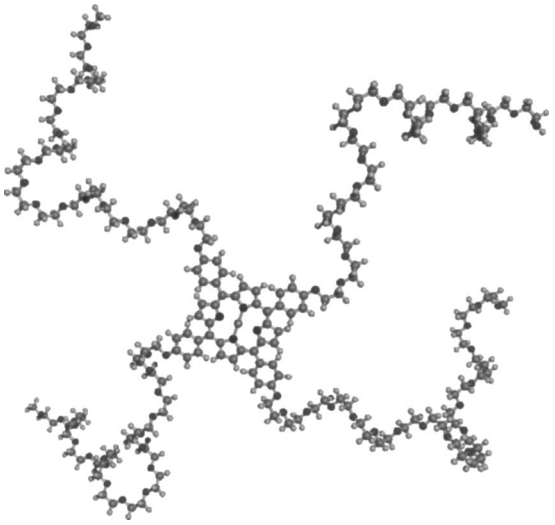

FIG. 1. 3D balls and sticks schematic representation of [5,10,15,20-tetra-*p*(ω-methoxy-polyethylenoxyphenyl)]metal porphyrin, where "metal" can be 2H, zinc, or cobalt atom.

criminator was also sent to a universal counter (Hewlett-Packard 53131 A), to perform all steady-state fluorescence measurements. The collected data were then analyzed using the nonlinear least-squares iterative reconvolution procedures based on the Marquardt algorithmn [23]. In the case of total fluorescence decay curves, the fitting was performed on the basis of the multiexponential decay law [24],

$$I(t) = I_0 \sum_i \alpha_i \exp(-t/\tau_i), \tag{1}$$

where $I(t)$ is total fluorescence decay curve, I_0 is the intensity at time zero, and α_i and τ_i are, respectively, the relative amplitude and lifetime of the ith component (the normalization condition is $\Sigma_i \alpha_i = 1$). In the case of time-resolved anisotropy measurements, the reconvolution fitting procedure was based on two steps [24]. Fluorescence anisotropy $[r(t)]$ is defined using the following expression:

$$r(t) = \frac{I_{VV}(t) - I_{VH}(t)}{I_{VV}(t) + 2I_{VH}(t)} = \frac{D(t)}{S(t)}, \tag{2}$$

where the sum data, $S(t)$, must be equal to the total intensity $I(t)$. In the first step, $S(t)$ was analyzed using a reconvolution procedure based on a multiexponential model [see Eq. (1)], to obtain the parameters describing the intensity decay (α_i and τ_i): in our experimental conditions, the parameters obtained by both the sum data and total intensity analysis were very close to one another (the differences were within a few percent). In the second step, holding constant the parameters recovered from the first step, the difference $D(t)$ was analyzed considering a multiexponential decay of the anisotropy [24],

$$D(t) = S(t)r(t) = S(t)r_0 \sum_j g_j \exp(-t/\tau_{Rj})$$
$$= S(t) \sum_j r_{0j} \exp(-t/\tau_{Rj}), \tag{3}$$

where the parameters $r_0 = \Sigma_j r_{0j}$, τ_{Rj}, and g_j represent, respectively, the limiting anisotropy in the absence of rotational diffusion, the individual rotational correlation times, and the associated fractional amplitudes in the anisotropy decay ($\Sigma_j g_j = 1$). In the simple case of spherical molecules, each τ_{Rj} is related to the volume (V_j) of the rotating unit (or of the equivalent sphere) by the following equation [24]:

$$\tau_{Rj} = \frac{\eta V_j}{k_B T}, \tag{4}$$

where η is the microviscosity of the medium, T is the temperature in kelvins, and k_B is the Boltzmann constant. Finally, the decays of the parallel (I_{VV}) and perpendicular (I_{VH}) components of the emission were reconstructed using all the parameters obtained by the first two steps on the basis of the following expressions:

$$I_{VV} = \tfrac{1}{3} I(t)[1 + 2r(t)],$$

$$I_{VH} = \tfrac{1}{3} I(t)[1 - r(t)], \tag{5}$$

and, then, superimposed with the experimental data. In all cases, the goodness of fit was evaluated on the basis of the reduced chi-square values (typically close to 1 for all the decay curves) and of the weighted residuals plots, ensuring that the latter are randomly distributed.

A rather simple relation exists between steady-state anisotropy r_S, defined from the steady-state expression of Eq. (2), and time-resolved $r(t)$ fluorescence anisotropy,

$$r_S = \frac{\int_0^\infty r(t) I(t) dt}{\int_0^\infty I(t) dt} \tag{6}$$

as well as between the steady-state intensity and the decay time,

$$I_S = \int_0^\infty I_0 \exp[-t/\tau] dt = I_0 \tau. \tag{7}$$

Under these hypotheses and provided that both time-resolved fluorescence intensity and anisotropy have a single decay time, Perrin's equation holds,

$$r_S = \frac{r_0}{1 + \tau/\tau_R}, \tag{8}$$

which relates r_S with the dynamic parameters r_0, τ, and τ_R.

B. uv-visible

uv-visible spectra were recorded on a Shimadzu uv-1601 spectrophotometer at $T = 22\ ^\circ$C using an aqueous borate buffer (pH 9) as solvent and cuvette with 0.1 cm path length. All the absorption spectra of amino acids and insulin samples do not show any signals in the examined range (300–700 nm).

C. Circular dichroism

The circular dichroism spectra were collected using a JASCO J-500A spectropolarimeter, with a 150 W xenon lamp under nitrogen flux. The difference between the intensity of the left- and right-polarized light transmitted through the sample, $\Delta I = 2(I_L - I_R)/(I_L + I_R)$, was analyzed by a lock-in module to obtain the circular dichroism (CD) signal. The instrument was fully controlled by a PC computer and the CD signal was calibrated in order to obtain the ellipticity, θ (proportional to the difference between the absorbance values), by using a 0.06% aqueous solution of d-10-camphorsulfonate.

The measurements were performed at 22 °C and corrected for the contribution from cell and solvent.

III. RESULTS AND DISCUSSION

Initial uv-vis spectroscopic studies on aqueous solutions of aliphatic or aromatic AAs and both metal-free porphyrin

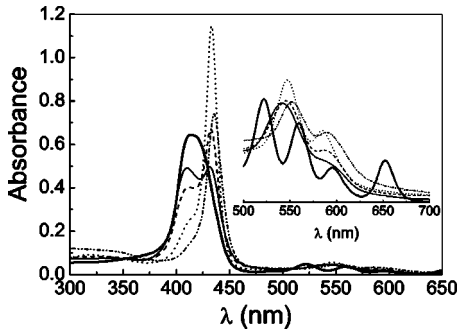

FIG. 2. uv-vis spectra of 2H-P (thick solid line), Co-P (solid line), and mixtures of Co-P with AAs: L-Ala (dashed line) in 1:10 molar ratio, L-Phe (dotted line) in 1:10 molar ratio, and insulin (dot-dashed line) in 1:1 molar ratio.

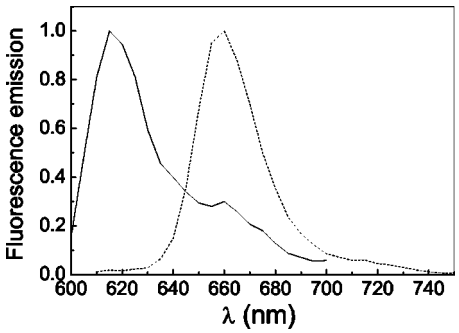

FIG. 3. Normalized fluorescence spectral distribution of 2H-P (dashed curve) and Co-P (solid curve) aqueous solutions.

(2H-P) and zinc-porphyrin (Zn-P) did not evidence any interaction between the porphyrin systems and the AAs. In fact, the uv-vis spectrum of the 2H-P (Fig. 2), constituted by a "Soret band" at 414.2 nm and four "*Q* bands" at 522.2, 560.0, 596.5 and 652.5 nm, and that of Zn-P, constituted by a "Soret band" at 431.4 nm and two "*Q* bands" at 561.1 and 604.7, remained unaffected by the addition of AAs solutions (spectra omitted for brevity).

Different data resulted when a cobalt-porphyrin (Co-P) was used. The uv-vis spectrum of an aqueous solution of the pure Co-P is shown in Fig. 2 (solid line). Two strong absorption bands, of comparable intensity, partially overlapped, appear at 410.5 and 432.0 nm. As reported by Pasternack *et al.* [25,26] for similar metal-porphyrin systems, these signals are explained considering that, in aqueous solutions, the cobalt atom can coordinate a different number of solvent molecules and/or ions, with a different interaction with the d metal-electrons and then different uv-vis absorption signals in the spectrum. For Co-P, the two "*Q* bands" appear at 541.6 and 588.8 nm.

Remarkably, important changes are observed (Fig. 2) in the Co-P spectrum when L-Ala, L-Phe, or Ins are added to its aqueous solution. In particular, a different increase of the intensity of the Soret band at 432 nm and a decrease of the intensity of the band at 410.5 nm can be noticed upon the AAs and protein addition. Furthermore, in the expanded traces of the *Q*-bands zone, reported in the inset of Fig. 2, it can be noted that all the signals are strongly redshifted with respect to those of pure Co-P system, depending on the AAs or insulin used. In particular, the deep changes observed in the absorption spectrum of Co-P/L-Phe or Ins are indicative of a greater interaction between the Co-P and aromatic AAs units, also when present inside the protein molecules, with respect to the aliphatic ones; this behavior could be useful for the construction of a selective AAs sensor.

In principle, the spectroscopic modifications observed above for the Co-P/AAs solutions could be alternatively attributed to the well-known porphyrin aggregation phenomenon [27–30]. This eventuality, however, has been excluded considering the results from dynamic light scattering experiments (photon correlation spectroscopy). In fact, the intensity autocorrelation function of Co-P (both in the absence and in the presence of AA) does not reveal any porphyrin aggregation phenomenon in a borate buffer solution (data not shown). Fluorescence spectra are shown in Fig. 3 for 2H-P and Co-P. The fluorescence spectrum of 2H-P, also in the presence of AAs, shows a maximum at 660 nm. Different data result when the cobalt atom is present: the fluorescence maximum shifts to 615–620 nm and, also in this case, the addition of AAs does not produce any changes in the fluorescence spectral distribution. In order to study in more detail the interaction phenomenon qualitatively revealed by uv-vis spectra, time-resolved fluorescence and time-resolved fluorescence anisotropy measurements were carried out.

The fluorescence decay of 2H-P (at 660 nm) shows a mono-exponential behavior, both in the presence and in the absence of AAs units, with a lifetime value of about 9 ns, as reported in Table I. The presence of the cobalt atom in the metal-porphyrin system induces a strong fluorescence quenching, probably due to the enhanced intersystem crossing to the triplet state. As showed in Fig. 4 and in Table I, the fluorescence decay of Co-P (at 615 nm) becomes bi-exponential, the lifetime values being 1.4 and 0.2 ns. The presence of AAs units does not induce significant variations in the fluorescence decay times (see Fig. 4: *A*, *B*, *C*, and *D* curves are almost parallel): the lifetime values are the same (1.4 and 0.2 ns) and, varying the amino acids, only the relative energy distributions ($\alpha\tau$) are different (see Table I). This circumstance also suggests that the photodynamic properties of Co-P probably do not change in the presence of AAs units. Interestingly, in the presence of the insulin, the fluorescence time decay is quite different (Fig. 4, curve *E* and Table I): the lifetime values significantly increase to 1.8 and 0.4 ns. In these conditions, the proteic structure seems to offer different microenvironments in which the chromophore molecules are more stabilized.

A more complex behavior is observed in the time-resolved fluorescence anisotropy measurements. In the absence of the cobalt atom, the fluorescence is completely depolarized [see Fig. 5(a)]. The zero anisotropy can only be due to the fact that the relative angle between the absorption and emission dipoles, in our conditions, is close to the magic angle (54.7 deg) to which corresponds a fundamental anisotropy value (r_0) equal to zero. In fact, a typical porphyrin moiety, in water solution, shows a rotational correlation time, τ_R, of about 0.5 ns [31], surely measurable with our instrumental apparatus. Moreover, in the present case, this rotational correlation time should be greater because of the pres-

TABLE I. Summary of the time-resolved fluorescence measurements.

Sample	$\tau_1 \pm 0.05$ (ns)	$\tau_2 \pm 0.05$ (ns)	$\alpha_1\tau_1$ (%)	$\alpha_2\tau_2$ (%)	$r_0 \pm 0.02$	$\tau_R \pm 0.05$ (ns)	$r_S \pm 0.02$
2H-P	9.2		100		0		0
2H-P/L-Trp	8.8		100		0		0
2H-P/L-Phe	8.8		100		0		0
Co-P	1.4	0.2	62	38	0.23	1.1	0.09
Co-P (aged)	1.4	0.2	64	36	0.23	1.1	0.10
Co-P/L-Ala	1.4	0.2	57	43	0.22	1.1	0.11
Co-P/L-Trp	1.4	0.2	72	28	0.18	1.5	0.11
Co-P/L-Phe	1.4	0.2	75	25	0.19	1.4	0.11
Co-P/L-Ala (aged)	1.4	0.2	50	50	0.23	2.0	0.10
Co-P/Ins	1.8	0.4	63	37	0.27	2.9	0.15

ence of PEGs groups. In the presence of the cobalt atom, both the steady-state and time-resolved fluorescence anisotropy are revealed. The anisotropy decay curves $[r(t)]$ are reported in Fig. 5, for Co-P solutions without amino acids (b) and in the presence of L-Ala (c), L-Trp (d), and Ins (e); whereas Fig. 6 shows, under the same conditions, the difference curves, $D(t)$, from which the anisotropy parameters (r_0 and τ_R, reported in Table I) are calculated by the best-fitting procedures, as explained in the experimental section.

First of all, it is important to note that the presence of the cobalt atom induces an r_0 value different from zero, which allowed us to measure a rotational correlation time of about 1.1 ns for Co-P.

The different behavior of the porphyrin fluorescence anisotropy, with and without the cobalt atom, is explained taking into account that, in the present conditions, the absorbing dipoles are different in the 2H-P and the Co-P systems. In fact, the used excitation wavelength (575 nm), in the case of Co-P, is close to the last "*Q* band," whereas this band is centered at 652.5 in the absence of the cobalt atom.

As reported in Table I, in the case of alanine the value of $\tau_R = 1.1$ ns was found, the same as that of Co-P, probably indicating that no interactions take place, under these conditions, between the alanine unit and the Co-P. On the contrary, when aromatic amino acids (tryptophane and phenyl-alanine) or insulin are added to the Co-P solutions, remarkable variations in the rotational correlation time are observed (1.4 ns for Co-P/Phe; 1.5 ns for Co-P/Trp; 2.9 ns for Co-P/Ins). This fact indicates that interactions occur between the cobalt-porphyrin star-polymer and the aromatic AAs units as well as the protein. Moreover, referring to Fig. 5(e), the anisotropy decay curve, in the presence of insulin, shows an apparent plateau of about 0.1, which could also correspond to a very long time component. In any case, this component is attributable to the binding of Co-P with some aggregated proteins, which significantly slows down the rotational dynamics of the Co-P molecules.

The τ_R values are coherent with the size of Co-P in different microenvironments ($\approx$2 nm). It is worth noting that a

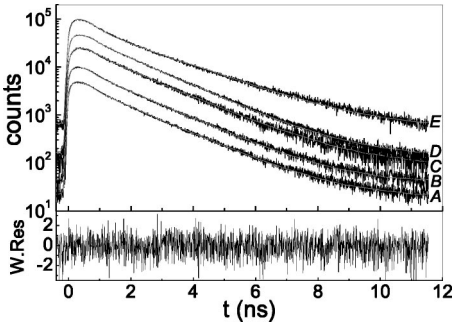

FIG. 4. Time-resolved fluorescence decay of *A*, Co-P (46 μM); *B*, Co-P/L-Ala (molar ratio 1:100); *C*, Co-P/L-Phe (molar ratio 1:100); *D*, Co-P/L-Trp (molar ratio 1:100); and *E*, Co-P/Ins (molar ratio 1:1). In order to make the graph more readable, each curve is scaled for a multiplicative factor (2, 5, 10, and 20, respectively). The lowest part of the plot shows the typical weighted residuals of the fit obtained with the reconvolution method ($\chi^2 = 1.08$).

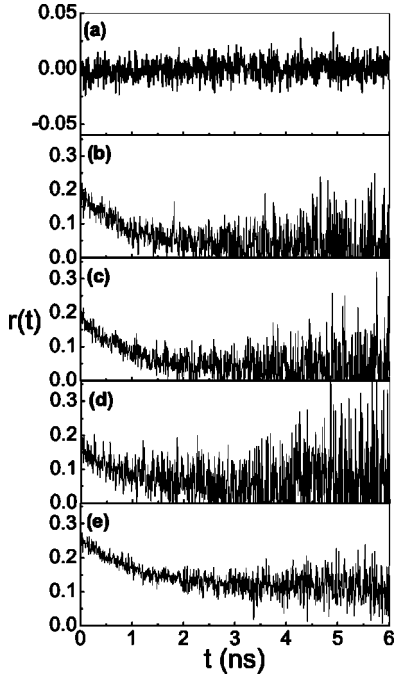

FIG. 5. Time-resolved anisotropy of (a) 2H-P (46 μM), (b) Co-P (46 μM), (c) Co-P/L-Ala (molar ratio 1:100), (d) Co-P/L-Trp (molar ratio 1:100), and (e) Co-P/Ins (molar ratio 1:1).

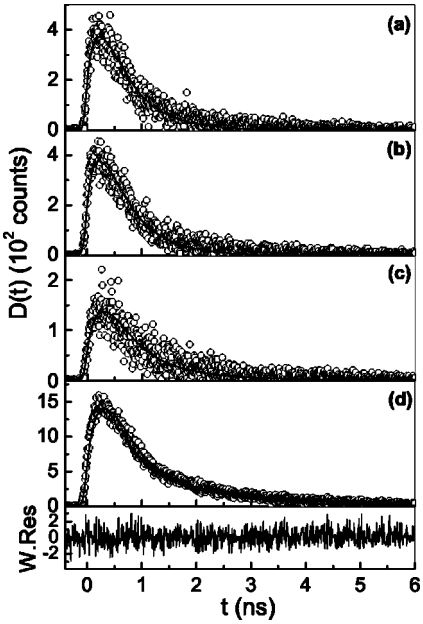

FIG. 6. Differences between parallel and orthogonal fluorescence decays together with the fit obtained using the reconvolution method: (a) Co-P, (b) Co-/L-Ala, (c) Co-P/L-Trp, and (d) Co-P/Ins. The lowest part of the plot shows the typical weighted residuals of the fit ($\chi^2=0.90$).

small mass change, due to the binding process, is successfully revealed by a significant change in τ_R [corresponding to a size variation within 10%, as calculated from Eq. (4)].

Surprisingly, in the case of aliphatic amino acid (alanine), an aging process (typically after one day) causes a significant change in the anisotropy decay curve $[r(t)]$ (see Fig. 7), showing a τ_R value of about 2 ns. No change is, instead, observed in the Co-P aged sample. This fact indicates that also aliphatic AAs units interact with the Co-P, but in this case the phenomenon includes kinetic processes which require a longer time scale.

As can be seen, time-resolved measurements, different from the steady-state ones (see Table I), allow for the discrimination of the interaction between Co-P and AAs. However, the steady-state anisotropy agrees with the dynamic quantities (r_0, τ, and τ_R) through Perrin's equation, where average values are used.

To further investigate the association of the chiral amino acids with the achiral Co-P, which causes an induced circular

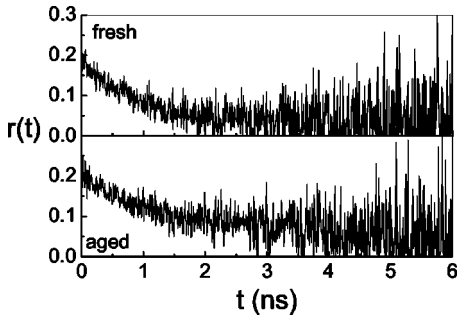

FIG. 7. Time-resolved anisotropy of Co-P/L-Ala freshly prepared and aged solution.

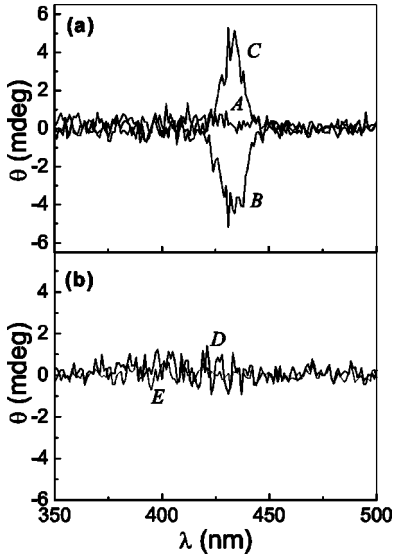

FIG. 8. CD spectra of the Co-P/phenylalanine. (a) *A*, Co-P; *B*, Co-P/L-Phe; and *C*, Co-P/D-Phe. (b) CD spectra of *D*, 2H-P and *E*, 2H-P/L-Phe.

dichroism (ICD), the CD technique has been employed as a sensitive analytical tool. An ICD band, in fact, appears within the absorption bands of the Co-P-based star polymer. In Fig. 8(a), the CD spectra for Co-P/Phe complex (analogous results were obtained for Co-P/Trp) are reported. It turns out that an ICD band appears at 434 nm, in correspondence to the Soret band of the porphyrin. The fact that the sign of the ICD band depends on the sign of chirality of the amino acid is a further validation that a chirality induction takes place. The presence of alanine, on the other hand, does not induce any ICD signal in the freshly prepared solution. In analogy with what is found by time-resolved fluorescence anisotropy measurements, the aged sample shows an ICD signal. The higher hydrophilicity of the alanine and, therefore, its tendency to remain in the solvent, could be responsible to this behavior.

Performing the same measurements on the star polymer 2H-P, which does not possess the cobalt atom, the ICD band does not appear either in the fresh or aged solution, as shown in Fig. 8(b). Co-P acts, therefore, as a recognition host by means of the coordination site of the cobalt of the core.

A binding (host)metal-N(guest) in complexes amino acid esters–metal porphyrins in $CHCl_3$ was hypothesized by Mizutani *et al.* [32,33] as the origin of the different type of ICD bands. For charged metalloporphyrins in water, on the other hand, some authors [6,34] revealed that a competition by the solvent in the coordination binding with the metal atom decreases the binding constant.

In the present case, in which the porphyrin-based star polymer is uncharged, the binding of the amino acids with the porphyrin core can be attributed to the concomitant presence of the coordination bond of the amino group with the metal atom and of the hydrophobicity effect. Moreover, against these circumstances favorable to the stabilization of the complex, the competitive binding affinity of water or buffer ions can act, but it seems to have only a marginal effect.

The binding between the Co-P and insulin is a more complex issue. The amino acid sequence and the conformation of the protein does not allow for an unambiguous and definitive assignement of the interaction sites. However, it seems quite plausible that the Co-P can interact with the insulin surface where hydrophobic patches are present. Moreover, the steric interaction by the PEG arms does not seem to hinder the binding with insulin.

On the basis of the results presented in this work, it turns out that, in water solution, besides the Co-N coordination, the contribution of the aromatic residues plays a crucial role in the recognition process of the Co-P.

IV. CONCLUSION

A binding process occurs between aromatic amino acids (and protein) and cobalt-porphyrin, made water-soluble by the presence of polyethylene glycol arms as substituents. The presence of a strong interaction is put in evidence by uv-vis, time-resolved fluorescence anisotropy, and ICD measurements. On the contrary, the study on Co-P/L-Ala solutions does not indicate a significant interaction between Co-P and the aliphatic AA: no changes in the rotational correlation time and no ICD signal are revealed. The fact that a binding with the aliphatic AA is revealed only after a very slow kinetic process suggests that, although the metal-N coordination bond is the common requisite for interaction, a preferential interaction with aromatic groups exists there.

Further studies, changing, for example, pH of solutions or using amino acid derivatives with amide group, are in progress in order to affect the coordination with the cobalt atom.

The porphyrin-based star polymer studied in the present work constitutes a fundamental starting point for creating new materials of relevant interest in the sensor fields and in bioscience. The solubility in water in the absence of electric charges, in fact, excludes the possibility of any electrostatic interaction and allows for a more selective discrimination of the binding process with respect to what happens for charged porphyrins.

[1] P. P. Pompa, A. Biasco, R. Cingolani, R. Rinaldi, M. Ph. Verbeet, and G. W. Canters, Phys. Rev. E **69**, 032901 (2004).

[2] C. Czeslik, R. Jansen, M. Ballauff, A. Wittemann, C. A. Royer, E. Gratton, and T. Hazlett, Phys. Rev. E **69**, 021401 (2004).

[3] F. Caruso, R. A. Caruso, and H. Mohwald, Science **282**, 1111 (1998).

[4] M. A. Awawdeh, J. A. Legako, and H. J. Harmon, Sens. Actuators B **91**, 227 (2003).

[5] Y. Aoyama, A. Yamagishi, M. Asagawa, H. Toi, and H. Ogoshi, J. Am. Chem. Soc. **110**, 4076 (1988).

[6] T. Mizutani, K. Wada, and S. Kitagawa, J. Am. Chem. Soc. **121**, 11425 (1999).

[7] E. Mikros, F. Gaudemer, and A. Gaudemer, Inorg. Chem. **30**, 1806 (1991).

[8] C. Verchere-Beaur, E. Mikros, M. Perre-Fauvet, and A. Gaudemer, J. Inorg. Biochem. **40**, 127 (1990).

[9] V. V. Borovkov, J. M. Lintuluoto, and Y. Inoue, J. Am. Chem. Soc. **123**, 2979 (2001).

[10] E. D. Sternberg, D. Dolphin, and C. Bruckner, Tetrahedron **54**, 4151 (1998).

[11] E. S. Nyman and P. H. Hynninen, J. Photochem. Photobiol., B **73**, 1 (2004).

[12] G. Jori, J. Photochem. Photobiol., B **36**, 87 (1996).

[13] E. Zenkevich, E. Sagun, V. Knyukshto, A. Shulga, A. Mironov, O. Efremova, R. Bonnett, S. P. Songca, and M. Kassem, J. Photochem. Photobiol., B **33**, 171 (1996).

[14] H. B. Ris, T. Krueger, A. Giger, C. K. Lim, J. C. M. Stewart, U. Althaus, and H. J. Altermatt, Br. J. Cancer **79**, 1061 (1999).

[15] S. Aime, M. Botta, E. Gianolio, and E. Terreno, Angew. Chem., Int. Ed. **39**, 747 (2000).

[16] S. A. Priola, A. Raines, and W. S. Caughey, Science **287**, 1503 (2000).

[17] G. Anneheimherbelin, M. Perreefauvet, A. Gaudemer, P. Helissey, S. Giorgirenault, and N. Gresh, Tetrahedron Lett. **34**, 7263 (1993).

[18] Y. X. Ci, Y. G. Zheng, J. K. Tie, and W. B. Chang, Anal. Chim. Acta **282**, 695 (1993).

[19] C. Vercherebeaur, M. Perreefauvet, E. Tarnaud, G. Anneheimherbelin, N. Bone, and A. Gaudemer, Tetrahedron **52**, 13589 (1996).

[20] N. Micali, V. Villari, P. Mineo, D. Vitalini, E. Scamporrino, V. Crupi, D. Majolino, P. Migliardo, and V. Venuti, J. Phys. Chem. B **107**, 5095 (2003).

[21] P. Mineo, E. Scamporrino, and D. Vitalini, Consiglio Nazionale delle Ricerche, Universita' di Catania, Patent and Appl. No. MI2004A001135.

[22] D. V. O'Connor and D. Phillips, *Time-Correlated Single Photon Counting* (Academic Press, New York, 1984).

[23] D. W. Marquardt, J. Soc. Ind. Appl. Math. **11**, 431 (1963).

[24] J. R. Lakowicz, *Principles of Fluorescence Spectroscopy* (Kluwer Academic/Plenum Publishers, New York, 1999).

[25] R. F. Pasternack, L. Francesconi, D. Raff, and E. Spiro, Inorg. Chem. **30**, 2606 (1973).

[26] R. F. Pasternack, E. Spiro, and M. Teach, J. Inorg. Nucl. Chem. **36**, 599 (1974).

[27] K. Kano, K. Fukuda, H. Wakami, R. Nishiyabu, and R. F. Pasternack, J. Am. Chem. Soc. **122** 7494 (2000).

[28] R. F. Pasternack, L. Francesconi, D. Raff, and E. Spiro, Inorg. Chem. **12**, 2606 (1973).

[29] N. Micali, F. Mallamace, A. Romeo, R. Purrello, and L. Monsu' Scolaro, J. Phys. Chem. B **104**, 5897 (2000).

[30] M. A. Castriciano, A. Romeo, V. Villari, N. Micali, and L. M. Scolaro, J. Phys. Chem. B **107**, 8765 (2003).

[31] N. C. Maiti, M. Ravikanth, S. Mazumdar, and N. Periasamy, J. Phys. Chem. **99**, 17 192 (1995).

[32] T. Mizutani, T. Ema, T. Yoshida, Y. Kuroda, and H. Ogoshi, Inorg. Chem. **32**, 2072 (1993).

[33] T. Mizutani, T. Ema, T. Yoshida, T. Renne, and H. Ogoshi, Inorg. Chem. **33**, 3558 (1994).

[34] T. Mizutani, K. Wada, and S. Kitagawa, J. Org. Chem. **65**, 6097 (2000).